

심실세동에서 흥분파의 분열 기전

Cedars -Sinai³,¹ UCLA,²
 이문형¹ · Zhilin Qu² · James N Weiss² · Alan Garfinkel²
 Hrayr S Karagueuzian³ · Peng-Sheng Chen³

Wavebreak Mechanism during Ventricular Fibrillation in Isolated Swine Right Ventricle

Moon-Hyoung Lee, MD¹, Zhilin Qu, PhD², James N Weiss, MD², Alan Garfinkel, PhD²,
 Hrayr S Karagueuzian, PhD³ and Peng-Sheng Chen, MD³

¹Cardiology Division, Yonsei Cardiovascular Hospital, College of Medicine, Yonsei University, Seoul, Korea,
²Division of Cardiology, Departments of Medicine, Physiology and Physiological Science,
 UCLA School of Medicine, Los Angeles, ³Division of Cardiology, Department of Medicine,
 Cedars-Sinai Medical Center, Los Angeles, California, USA

ABSTRACT

Background : Several different patterns of wavebreak have been described by mapping of the tissue surface during fibrillation. However, it is not clear whether these surface patterns are caused by multiple distinct mechanisms or by a single mechanism. **Method** : To determine the mechanism by which wavebreaks are generated during ventricular fibrillation, we conducted optical mapping studies and single cell transmembrane potential recording in 6 isolated swine right ventricles. **Results** : Among 763 episodes of wavebreak (0.75 times/sec/cm²), optical maps showed 3 patterns : 80% due to a wavefront encountering the refractory waveback of another wave, 11.5% due to wavefronts passing perpendicularly each other and 8.5% due to a new (target) wave arising just beyond the refractory tail of a previous wave. Computer simulations of scroll waves in 3-D tissue showed that these surface patterns could be attributed to two fundamental mechanisms : head-to-tail interactions and filament break. **Conclusion** : We conclude that during sustained ventricular fibrillation in swine RV, surface patterns of wavebreak are produced by two fundamental mechanisms : head-to-tail interaction between waves and filament break. (**Korean Circulation J 2000;30(11):1404-1416**)

KEY WORDS : Reentry · Mapping · Electrophysiology · Action potentials · Restitution.

서 론

multiple wavelet hypothesis

wavelet

wavelet

Moe¹⁾

(wave splitting)가

: 2000 11 20

: 2000 12 19

: , 120 - 752 134

: (02) 361 - 7071, 7084 · : (02) 393 - 2041 E - mail : mhlee@yumc.yonsei.ac.kr

daughter wavelet

2-4) 5-7) multiple wavelet

(activation map)

break 가 가 wave -

ve가 7)8) 9) wa -

10)11) wavefront가

wavetail wavebreak

wavefront - wavetail 8)

wavebreak 10)11)

vebreak wa -

12) 가 6)

가 3 가

재료 및 방법

실험조직과 광학적 지도화

6 (20 30 kg) pentothal sodium
30 mg/kg

3

4 Tyrode (NaCl, 125.0 ; KCl, 4.5 ; MgCl₂,
0.5 ; CaCl₂, 0.54 ; NaH₂PO₄, 1.2 ; NaHCO₃, 24.0 ;
glucose, 5.5(mM/l) ; albumin, 50 mg/l)

6 - F polyethylene
95% 가
Tyrode 15 cc

3 - 0 silk Tyrode
Tissue bath
tissue bath
Tissue bath
가 36.5
95% 가 37 Tyrode

1
μmol/l pyrimidine 4 - (2 - (6 - (dibutylamino) - 2 -
naphthalenyl) - 1 - (3 - sulfopropyl) hydroxide(di - 4 -
ANEPPS, Molecular Probes, Inc) 20

(glass electrode)

2)
12) 510 ± 40 nm
band - pass filter 250 - W tungsten - ha -
logen lamp(Model 66196, Oriel Corp., Stratford, CT,
USA) 600
nm long - pass filter(R60, Nikon, Tokyo, Japan)
25 mm/f 0.85 video lens(Fujinon CF25L,
Fuji Photo Optical Co., Omiya City, Japan)

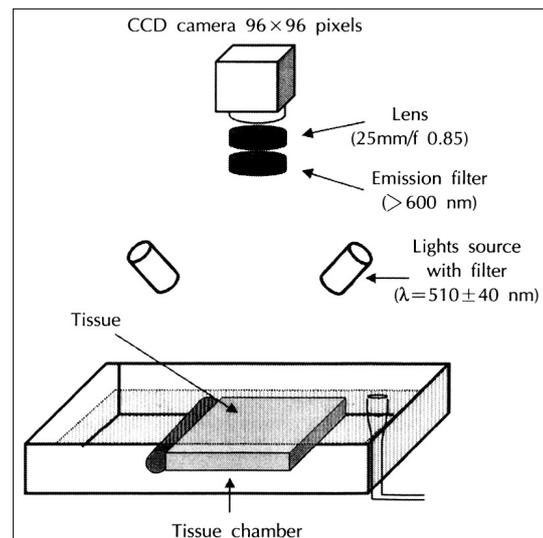


Fig. 1. Optical mapping setup. Schematic diagram of optical mapping apparatus. See text for details.

12bit digital charge coupled device(CCD : CA - D1 - 0256T, Dalsa Inc., Ontario, Canada)

(Fig. 1). shutter 3.75 ms
96 x 96 pixel
frame grabber(IC - PCI - DIG16, Imaging Technology, Bedford, MA, USA)가

tis -
sue bath
(Excitation - Co -
ntraction uncoupler)

형광신호처리

5 pixel
median
255
0 pixel
0.27mm 0.68 mm

3
3 °/m)

3 (scroll wave)
San Diego supercomputer center

pixel 256 gray scale

wavebreak
wavefront waveback
wavebreak

wavefront wave -
back¹³⁾

wavebreak
wavebreak
mosaic

frame
wavebreak
wavebreak

frame wavefront isochronal
map

활동전위

90% (APD₉₀) (diastolic interval : DI)

(action potential duration restitution curve ; APDR curve) APD₉₀ DI

ORIGIN 5.0(Microcal Software, Inc., Northampton, MA, USA) exponential fitting⁶⁾

컴퓨터 모의실험

3
Luo - Rudy Phase 1
restitution

no flux boundary condition¹⁴⁾
0.02 0.2 ms , 0.015 cm

(1)
¹⁸⁾ 가 4.8 x 4.8 x 0.9 cm
(fiber) 120 ° (= 13.

3 °/m)
3 (scroll wave)

San Diego supercomputer center

통계처리
ORIGIN(Microcal Software, Inc., Northampton, MA, USA)

±
Student t - test . p

0.05

결 과

실세동에서 활동전위 기간복원성(Action potential duration restitution)

AP -
DR , DI APD₉₀
79 ± 17 ms DI 12 ±

8 ms Fig.
2A APDR curve

(Fig. 2B). 2.4 7.6

광학적 지도로 본 심실세동시 Wavebreak

multiple wavelet		wavebreak		흥분파의 수직충돌에 의한 Wavebreak	
83	763	86	(11%)	7)	Fig. 5
0.75	612	wav -	wavebreak	wavefront가	
ebreak	wavefront가				
Fig. 3		가	Fig. 5		Fig. 6
3		(Fig. 3, fr -			isochronal map(panel B)
ame b)	wavelet	wavebreak	Waveback에서 기원한 Wavefront		
	Fig. 9	(65 (8.5%)	wav -	
)	wavelet	elet			
Fig. 4C	Fig. 3	Fig. 9	isochr -		
onal map	Wavebreak	(1 - 6)	wavebreak	(Fig. 7).	
(a - f)	panel A, B	가	Wavebreak 근처에서의 활동전위 양상		
		가	Wavebreak		
(panel D). Panel A					wav -
wavebreak		ebreak	2 mm		

Table 1. Computer simulation equation

The partial differential equation for cardiac conduction is¹⁴⁾:

$$\nabla \cdot \tilde{D} \nabla V = -I_{ion}/C_m + \nabla \cdot \tilde{D} \nabla V \quad (1)$$

where V is the TMP and C_m the membrane capacitance. I_{ion} is the total ionic current density of the membrane. $\tilde{D} = \tilde{\sigma}/S_v C_m$ is the diffusion tensor, where $\tilde{\sigma}$ is the conductivity tensor and S_v the surface-to-volume ratio of the cell. We use no flux boundary condition¹⁴⁾: $\tilde{n} \cdot (\tilde{D} \nabla V) = 0$, where \tilde{n} is the unit vector normal to the boundary. We assume the fibers are parallel and uniform in the x-y plane but rotate along the z-direction. Therefore, \tilde{D} has the following matrix structure¹⁴⁾:

$$\tilde{D} = \begin{pmatrix} D_{xx} & D_{yx} & 0 \\ D_{xy} & D_{yy} & 0 \\ 0 & 0 & D_{zz} \end{pmatrix}$$

where

$$\begin{aligned} D_{xx} &= D \cos^2 \theta(z) + D_a \sin^2 \theta(z) \\ D_{yy} &= D \sin^2 \theta(z) + D_a \cos^2 \theta(z) \\ D_{xy} &= D_{yx} = (D - D_a) \sin \theta(z) \cos \theta(z) \\ D_{zz} &= D_a \end{aligned} \quad (3)$$

D is the diffusion constant along the fiber direction, and D_a is the transverse diffusion constant. We use $D = 0.001 \text{ cm}^2/\text{ms}$ and $D_a = 0.0002 \text{ cm}^2/\text{ms}$. $\theta(z)$ is angle between the fiber and the x-axis. We use a uniform fiber rotation angle $\theta(z) = \alpha z$ with α being a constant. I_{ion} in Eq. (1) is taken from the LR1 AP model.¹⁷⁾ We varied some parameters to change the APD and APD restitution. The parameters were selected so that APD restitution was steep enough to cause spontaneous wave break in the simulated 3D tissue when the thickness exceeded 0.4 cm. We used $\tilde{G}_{NZ} = 16 \text{ mS}/\text{cm}^2$, $\tilde{G}_K = 0.0423 \text{ mS}/\text{cm}^2$ and $\tilde{G}_{si} = 0.047 \text{ mS}/\text{cm}^2$. We also sped up the Ca^{2+} kinetics: i.e., $\tau_d = 0.5 \tau_d$ and $\tau_f = 0.5 \tau_f$.

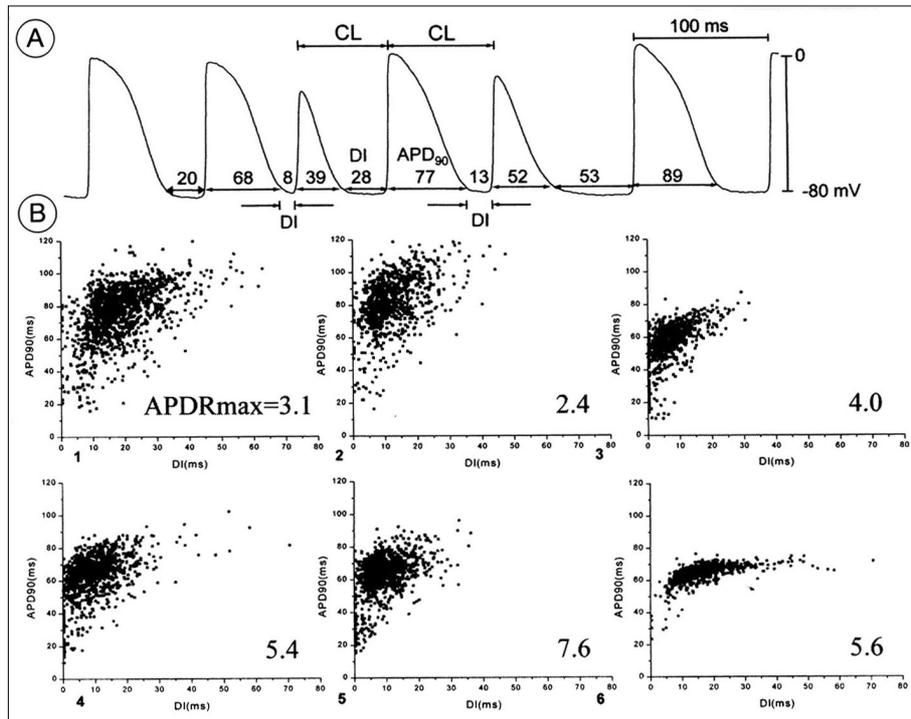


Fig. 2. AP recorded during VF and APD restitution curves during VF in 6 isolated swine RV. Panel A is a typical TMP recording showing that APD is positively related to the preceding DI. Panel B shows APD restitution characteristics in all six tissues. APDR max, the maximum slope of the APD restitution curve, is identified by numbers in each of the 6 tissues. CL = cycle length.

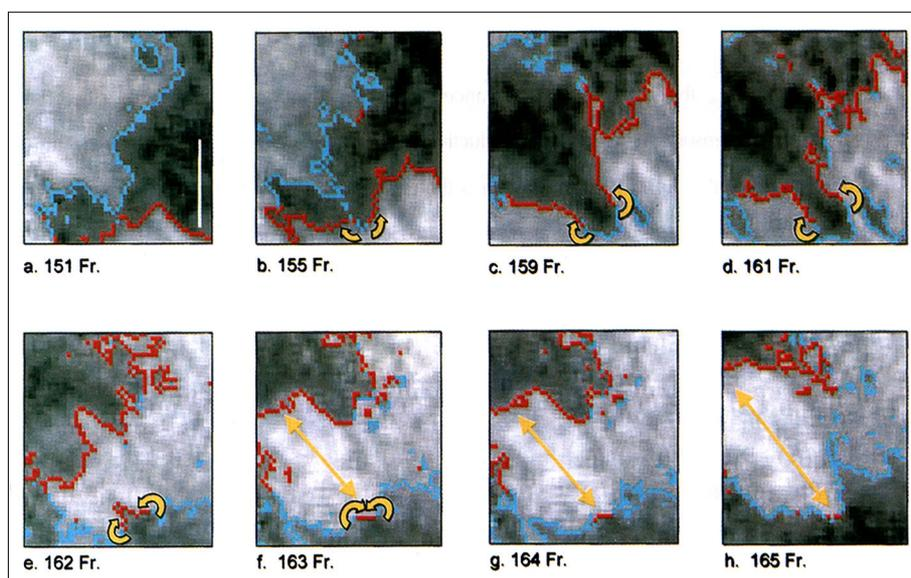


Fig. 3. The wavebreak and initiation of reentry by a wavefront encountering the trailing edge of refractoriness from a neighboring wave. Shown are sequential wave maps recorded by the optical mapping system during VF. The red line denotes the wavefront and the blue line the wave tail. Curved yellow arrows indicate the direction of the reentrant wavefronts. The double headed yellow arrow draws attention to two waves traveling in opposite directions. The vertical white bar at the right lower corner of frame a is 1 cm long.

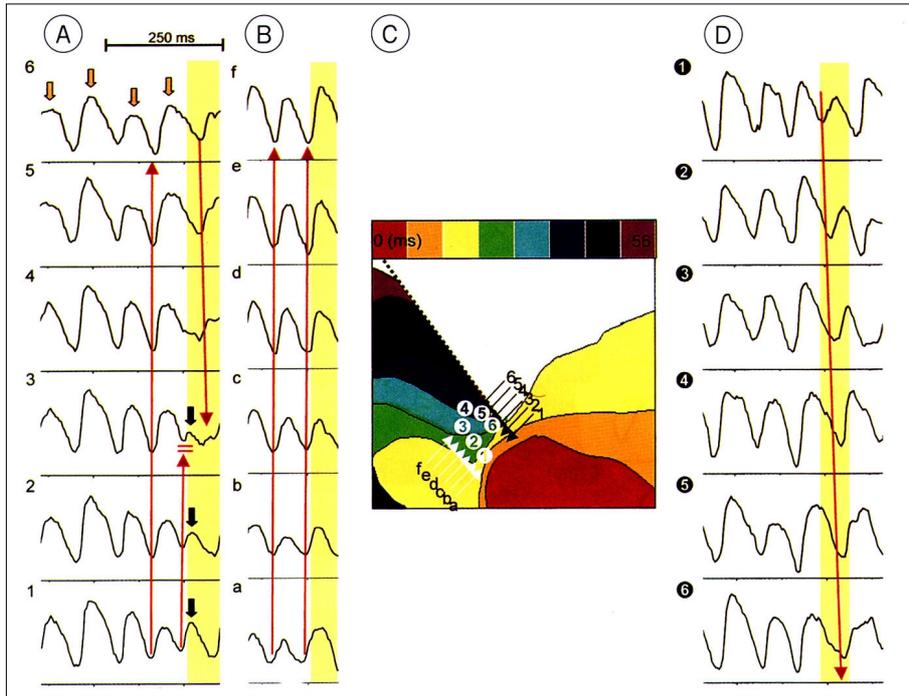


Fig. 4. Isochronal map (C) and optical potentials (A, B and D) of wavebreak. This is the same episode as that shown in Fig. 3. The upper portion of Panel C shows an isochronal map with arrows pointing to the two wavebreak sites. The lower portion of Panel C shows the same isochronal map with numbers and letters corresponding to the recordings shown in panels A, B and D. The yellow segments in A, B and D indicate the time window during which the activations in frames a to h of Fig. 3 were registered.

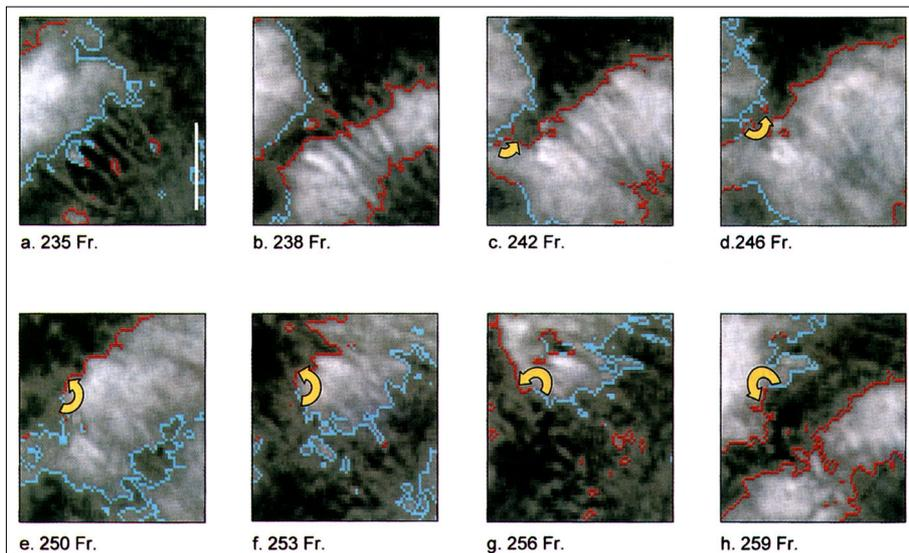


Fig. 5. The wavebreak and initiation of reentry by perpendicular interaction of two wavefronts. Shown are sequential dynamic wave maps of activation and repolarization. The red line represents the wavefront ; the blue line shows the refractory wave tail.

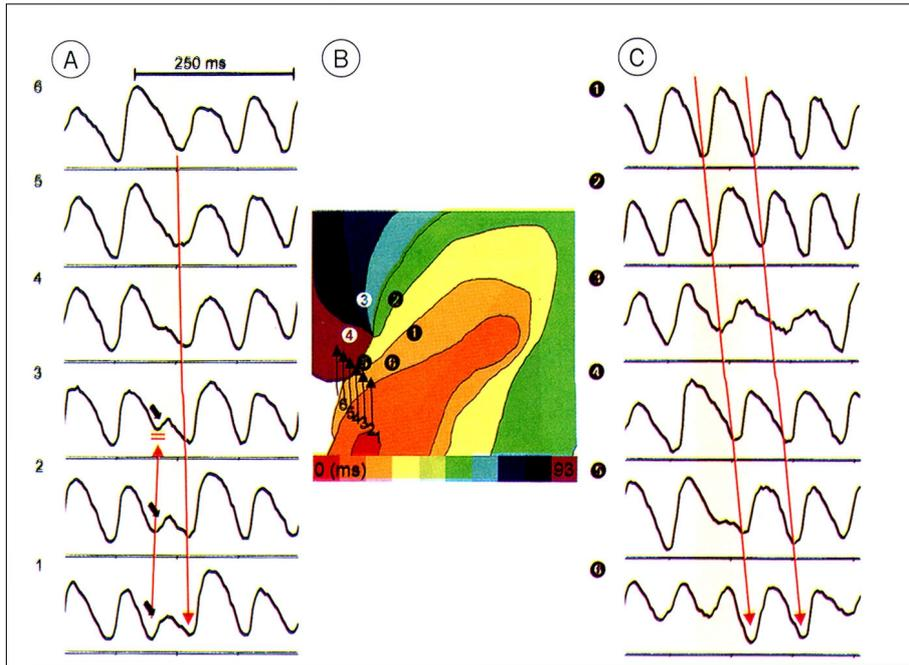


Fig. 6. Isochronal map (B) and optical signals (A and C) of wavebreak associated with the perpendicular interaction of two waves. This is the same episode as that shown in Fig. 5. The arrow in the upper isochronal map in Panel B shows the site of wavebreak. The lower portion of Panel B shows the same isochronal map with numbers and letters corresponding to the recordings shown in panels A and C. The yellow segments in panels A and C indicate the time window during which the activations in frames a to h of Fig. 5 were registered.

(action potential amplitude), APD 90, (dV/dt) max, DI 54 ± 16 mV, 62 ± 16 ms, 33 ± 19 V/s and 11 ± 8 ms . 5 wavebreak (2 mm) (Fig. 8) 10)⁷⁾ 가 wav - parameter 31 ± 15 mV, 36 ± 13 ms, 11 ± 7 V/s, 5 ± 4 ms wavebreak filament) 3 (scroll daughter scroll

. wavebreak parameter 11) wavefront, waveback, wavebreak break (Fig. 11).¹⁹⁾

Discussion

3차원 가상 심장조직에서의 컴퓨터 모의실험

wavebreak Luo - Rudy Phase 1 (LR1) wavebreak (LR1) APDR curve (head) (tail) 가 3 가 (scroll filament) wavebr - wavebreak . eak Krinsky²⁰⁾

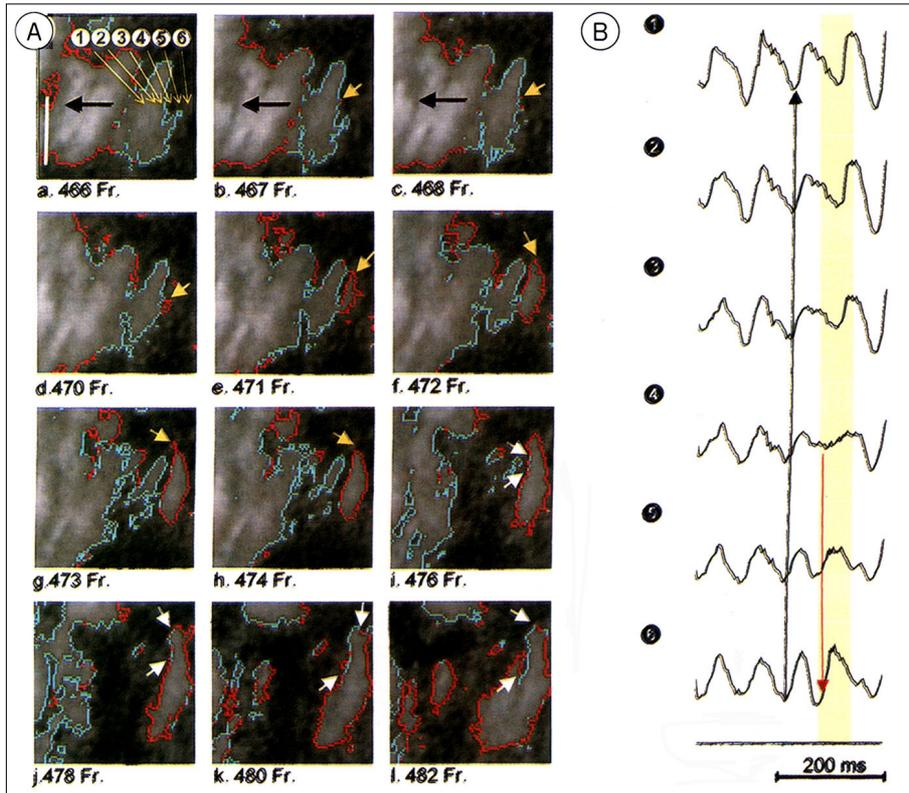


Fig. 7. Wavebreak occurring without wave-wave interaction. Panel A shows a wave propagating from right to left (black arrows). From the end of a previous waveback, a wavelet emerges and propagates in the opposite direction (yellow arrows) with new wavebreaks (white arrows). Panel B shows optical signals. The numbers correspond to the locations shown in panel A-a. The yellow segment in panel B indicates the time window during which the activations in frames a to i of panel A were registered.

Karma¹⁴⁾가 wavebreak Fenton () 24)
 심실세동의 유지기전 9) wavefront가 Gray
 Multiple wavelet hypothesis¹⁾ eak wavebr -
 wavebreak wavelet wavebreak restitution Gray 9)
 wavebreak (activation pattern) 21 - 23) (multiple electrode ma-
 wavebreak wavebreak 가 ping) 7)
 phase singularity 9) wavefront

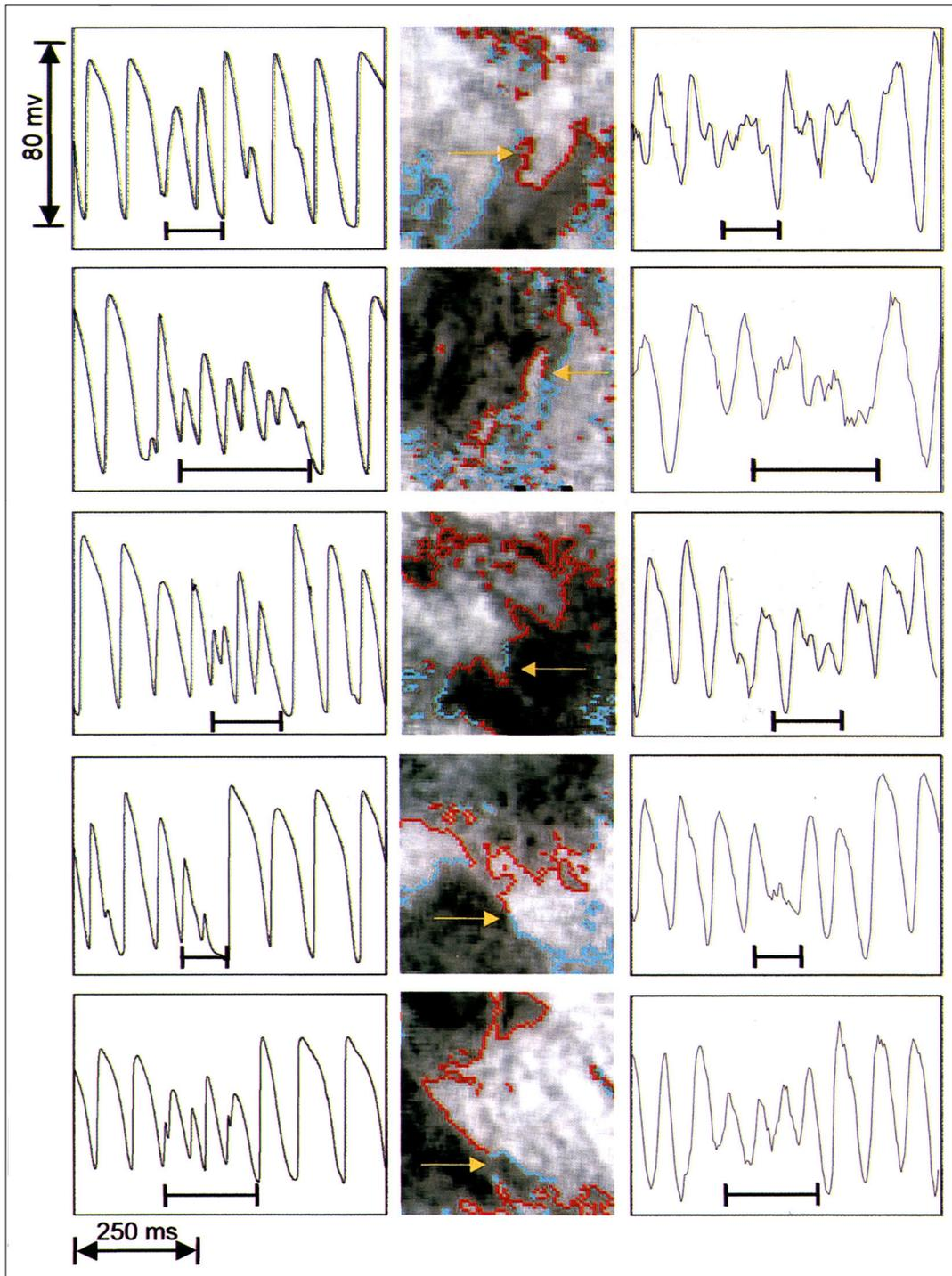


Fig. 8. Five examples of single cell TMP (left column) and simultaneously registered fluorescent signals (right column) at or near the wavebreak (middle column). Each of the five rows represents one episode. The line segment below each panel indicates the times when wavebreak and reentrant wavefronts were recorded by the optical mapping system. The yellow arrows point to the site where TMP and fluorescent signals were recorded in each episode.

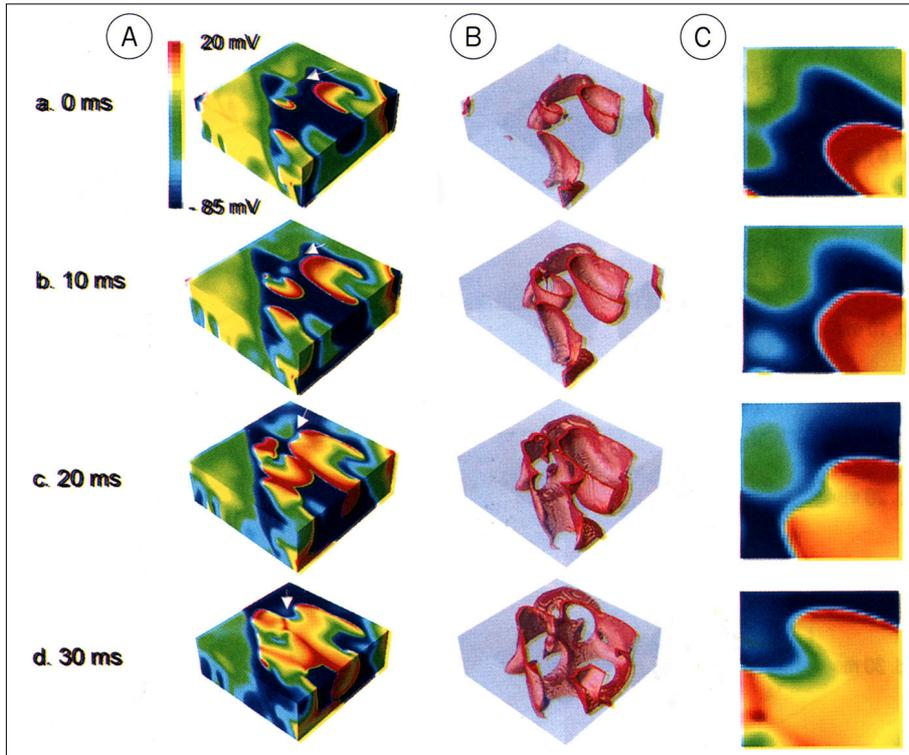


Fig. 9. 3-D simulation of wavebreak by a wavefront running into the trailing edge of refractoriness. Panel A shows the surface activation patterns (red = wavefront, green = waveback) at the times indicated. The white arrows indicate the region where this mechanism of wavebreak occurs. Panel B shows the corresponding scroll wavefronts in the tissue (red = rising membrane voltage). Panel C is a blow-up of the region of wavebreak on the upper surface (near the white arrows in A). Residual refractoriness (green) was left over by a previous wavefront and when the next wave (red) encountered this refractory region, wavebreak occurred, generating two new scroll waves. Compare with the experimental wavebreak in Fig. 3.

흥분성의 회복과 Wavebreak의 기전

(異質性) APDR (scroll wave)²⁹⁾
 APD co -
 conduction velocity(CV) restitution¹⁶⁾
 APDR curve 가 가 연구목적 :
 1 (Fig. 2) 가 가 (activation map)
 가 1 가 1 가 wavebreak
 DI APD wave가
²⁶⁾ 가 1
²⁷⁾²⁸⁾ APD wavefront가
 safety factor가 wavetail wavebreak
 wavebreak . Fig. 4A wavebreak
 wavebreak 가
 restitution hypothesis

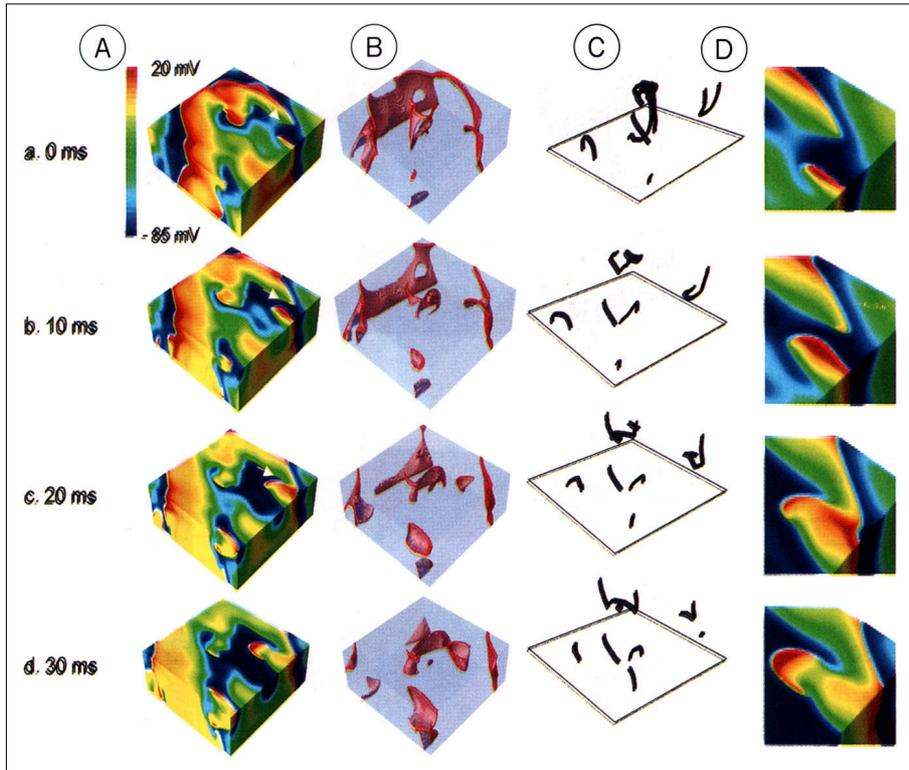


Fig. 10. 3-D simulation of wavebreak by perpendicular intersection. As in Fig. 8, panels A-D show the surface activation patterns, the scroll wavefronts in the tissue, the filament and a blow-up of the region of wavebreak (near the white arrows in A), respectively. A wavefront propagates upward to the right, leaving an area of residual refractoriness at its waveback. A different wavefront propagates upwards from the left, perpendicular to the first wavefront. It encounters residual refractoriness, causing wavebreak and a new scroll filament to form. Compare with the experimental wavebreak in Fig. 5.

APDR curve 2.4 7.6
 가 2) multiple wa-
 3 velet
 가 3) 83 763 wavebreak
 방 법 : wavebreak , (cm²) 0.75
 612 wavefront wavetail
 , 86
 , 65
 waveb -
 reak ,
 LR1 supe - 4)
 rcomputer wavebreak 3 wavefront가
 결 과 : scroll filament가 가
 가
 1) 79 ± 17 ms 결 론 :
 DI 12 ± 8 ms wavebreak wave-

- in ventricular fibrillation. *Circ Res* 1994;74:495-506.
- 9) Gray RA, Pertsov AM, Jalife J. *Spatial and temporal organization during cardiac fibrillation. Nature* 1998;392:75-78.
 - 10) Davidenko JM, Salomonsz R, Pertsov AM, Baxter WT, Jalife J. *Effects of pacing on stationary reentrant activity. Theoretical and experimental study. Circ Res* 1995;77:1166-79.
 - 11) Pertsov AM, Davidenko JM, Salomonsz R, Baxter WT, Jalife J. *Spiral waves of excitation underlie reentrant activity in isolated cardiac muscle. Circ Res* 1993;72:631-50.
 - 12) Lin SF, Roth BJ, Wikswo Jr JP. *Quatrefoil reentry in myocardium: An optical imaging study of the induction mechanism. J Cardiovasc Electrophysiol* 1999;10:574-86.
 - 13) Mandapati R, Asano Y, Baxter WT, Gray R, Davidenko J, Jalife J. *Quantification of effects of global ischemia on dynamics of ventricular fibrillation in isolated rabbit heart. Circulation* 1998;98:1688-96.
 - 14) Fenton F, Karma A. *Vortex dynamics in three-dimensional continuous myocardium with fiber rotation: Filament instability and fibrillation. Chaos* 1998;8:20-47.
 - 15) Antzelevitch C, Jalife J, Moe GK. *Characteristics of reflection as a mechanism of reentrant arrhythmias and its relationship to parasystole. Circulation* 1980;61:182-91.
 - 16) Cao JM, Qu Z, Kim YH, Wu TJ, Garfinkel A, Weiss JN, et al. *Spatiotemporal heterogeneity in the induction of ventricular fibrillation by rapid pacing: Importance of cardiac restitution properties. Circ Res* 1999;84:1318-31.
 - 17) Luo CH, Rudy Y. *A model of the ventricular cardiac action potential. Depolarization, repolarization, and their interaction. Circ Res* 1991;68:1501-26.
 - 18) Qu Z, Garfinkel A. *An advanced algorithm for solving partial differential equation in cardiac conduction. IEEE Trans Biomed Eng* 1999;46:1166-8.
 - 19) Athill CA, Ikeda T, Kim YH, Wu TJ, Fishbein MC, Karagueuzian HS, et al. *Transmembrane potential properties at the core of functional reentrant wavefronts in isolated canine right atria. Circulation* 98:1556-67.
 - 20) Krinsky VI. *Spread of excitation in an inhomogeneous medium. Biophys J* 1966;11:776-84.
 - 21) Chen PS, Wolf PD, Dixon EG, Danieleley ND, Frazier DW, Smith WM, et al. *Mechanism of ventricular vulnerability to single premature stimuli in open-chest dogs. Circ Res* 1988;62:1191-209.
 - 22) Davidenko JM, Pertsov AM, Salomonsz R, Baxter W, Jalife J. *Stationary and drifting spiral waves of excitation in isolated cardiac tissue. Nature* 1992;355:349-51.
 - 23) Winfree AT. *Spiral waves of chemical activity. Science* 1972;175:634-6.
 - 24) Salzberg BM, Davila HV, Cohen LB. *Optical recording of impulses in individual neurones of an invertebrate central nervous system. Nature* 1973;246:508-9.
 - 25) Davidenko JM, Persow AV, Salomonza R, Baxter W, Jalife J. *Sustained vortex-like waves in normal isolated ventricular muscle. Proc Natl Acad Sci USA* 1990;355:349-51.
 - 26) Weiss JN, Garfinkel A, Karagueuzian HS, Qu Z, Chen PS. *Chaos and the transition to ventricular fibrillation: A new approach to antiarrhythmic drug evaluation. Circulation* 1999;99:2819-26.
 - 27) Karagueuzian HS, Khan SS, Hong K, Kobayashi Y, Denton T, Mandel WJ, et al. *Action potential alternans and irregular dynamics in quinidine-intoxicated ventricular muscle cells. Implications for ventricular proarrhythmia. Circulation* 1993;87:1661-72.
 - 28) Karma A. *Electrical alternans and spiral wave breakup in cardiac tissue. Chaos* 1994;4:461-72.
 - 29) Qu Z, Weiss JN, Garfinkel A. *Cardiac electrical restitution properties and stability of reentrant spiral waves: a simulation study. Am J Physiol* 1999;276:H269-H283.